Published in final edited form as:
Acta Biomater. 2021 November 01; 135: 663–670. doi:10.1016/j.actbio.2021.08.051.

Sclerites of the soft coral *Ovabunda macrospiculata* (Xeniidae) are predominantly the metastable $CaCO_3$ polymorph vaterite

Jeana L. Drake[1,+], **Yehuda Benayahu**[2], **Iryna Polishchuk**[3], **Boaz Pokroy**[3], **Iddo Pinkas**[4], **Tali Mass**[1,5,*]

[1]Department of Marine Biology, Leon H. Charney School of Marine Sciences, University of Haifa, Mt. Carmel, Haifa 3498838, Israel

[2]School of Zoology, George S. Wise Faculty of Life Sciences, Tel Aviv University, Tel Aviv 66798, Israel

[3]Department of Materials Science and Engineering and the Russel Berrie Nanotechnology Institute, Technion-Israel Institute of Technology, Haifa 32000, Israel

[4]Department of Chemical Research Support, Weizmann Institute of Science, Rehovot 7610001, Israel

[5]Morris Kahn Marine Research Station, The Leon H. Charney School of Marine Sciences, University of Haifa, Sdot Yam, Israel

Abstract

Soft corals (Cnidaria, Anthozoa, Octocorallia, Alcyonacea) produce internal sclerites of calcium carbonate previously shown to be composed of calcite, the most stable calcium carbonate polymorph. Here we apply multiple imaging and physical chemistry analyses to extracted and *in-vivo* sclerites of the abundant Red Sea soft coral, *Ovabunda macrospiculata*, to detail their mineralogy. We show that this species' sclerites are comprised predominantly of the less stable calcium carbonate polymorph vaterite (>95%), with much smaller components of aragonite and calcite. Use of this mineral, which is typically considered to be metastable, by these soft corals has implications for how it is formed as well as how it will persist during the anticipated anthropogenic climate change in the coming decades. This first documentation of vaterite dominating the mineral composition of *O. macrospiculata* sclerites is likely just the beginning of establishing its presence in other soft corals.

Abstract

[+]corresponding author during manuscript review, jeanadrake@g.ucla.edu, phone 001-415-7284724, fax 001-310-825-2779.
[*]corresponding author upon publication, tmass@univ.haifa.ac.il, phone 972-4-8288977, fax 9724-8288267.

6 **Author contributions**

YB and TM conceived the study, YB supplied the soft coral samples for sclerite preparation, TM conducted scanning electron microscopy analyses, IPi conducted Raman measurements and analyses, IPo and BP conducted HRPXRD measurements and analyses, and all authors analyzed the data. All authors wrote the manuscript and approved of this submission.

Declaration of interests

☒ The authors declare that they have no known competing financial interests or personal relationships that could have appeared to influence the work reported in this paper.

☐ The authors declare the following financial interests/personal relationships which may be considered as potential competing interests:

Europe PMC Funders Author Manuscripts

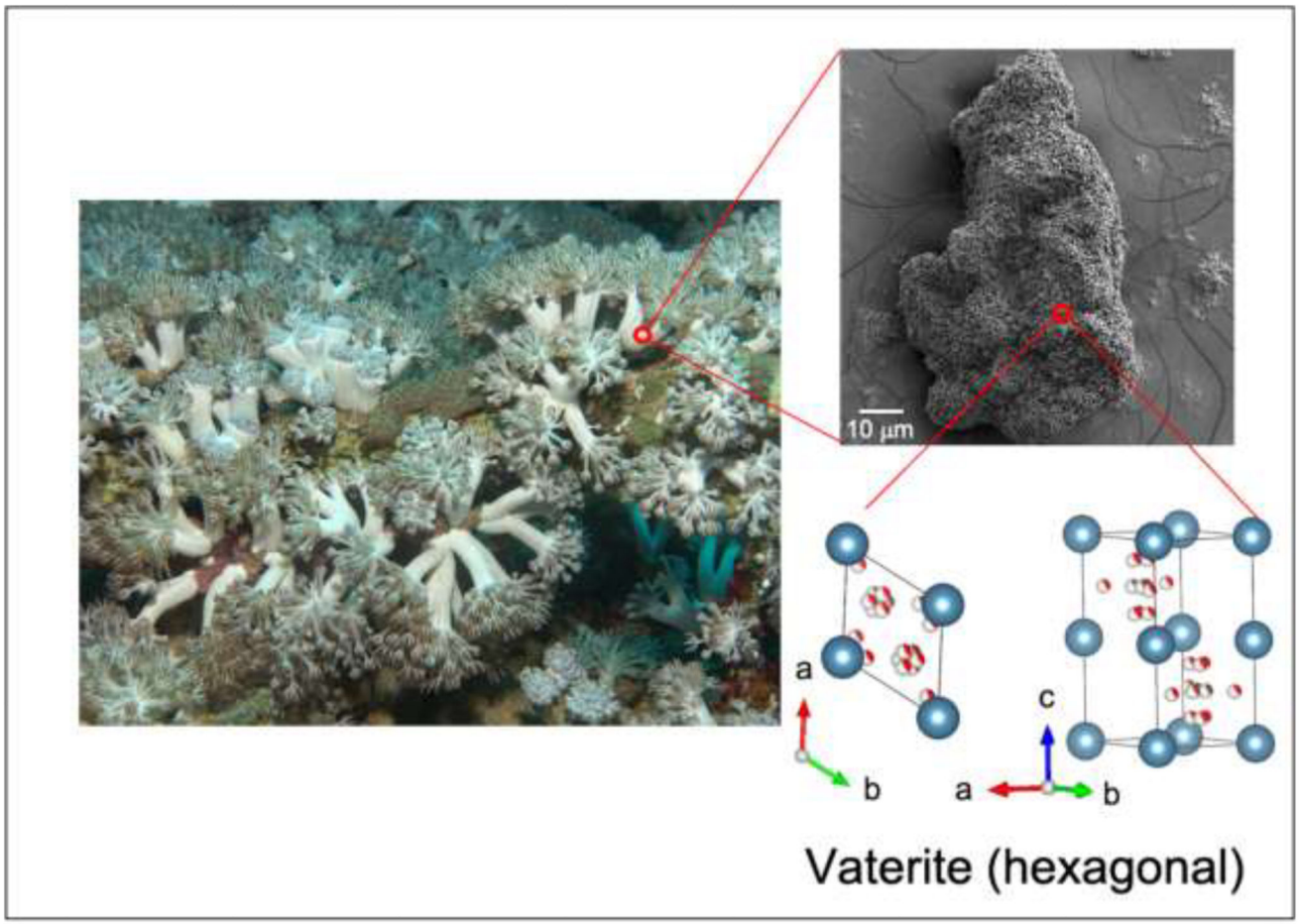

Graphical abstract.

Keywords

Calcium carbonate; micro-Raman spectroscopy; scanning electron microscopy; energy dispersive spectroscopy; high-resolution powder X-ray diffraction; Red Sea coral reefs; soft corals

1 Introduction

Cnidarians produce a wide variety of calcium-based biominerals [1], with the dominant type of calcification producing calcium carbonate in one of its polymorphs (i.e., one of several crystal structures of the same chemical formula). Some benthic hydrozoans such as lace corals produce relatively large aragonite or calcite structures [e.g., 2]. Within modern anthozoans, stony/scleractinian corals (Hexacorallia) and blue corals (Octocorallia) can produce large aragonite skeletons [3, reviewed by 4], while other octocorals including soft corals, gorgonians, precious corals, and sea pens produce calcite, Mg-calcite, and/or aragonite sclerites [5–8], with some hexacorals and octocorals also forming amorphous calcium carbonate (ACC) likely as a mineral precursor [5, 9]. As the negative effects of

ocean acidification on calcifying marine organisms become more evident in the coming decades [reviewed by 10], some, though clearly not all, calcifying anthozoans may find it harder to produce their calcium carbonate structures [e.g., 11, 12–14].

From a phylogenetic perspective, calcium carbonate polymorph presence (or lack of such structures) is not restricted to specific orders, growth forms, or photosymbiotic status within Anthozoa, and the ability to calcify appears to have arisen multiple times [15]. Further, several orders contain taxa that produce multiple minerals, much of which has only been revealed in recent years. For instance, among the calcifying hexacorals, stony corals have been shown to form amorphous calcium carbonate which dehydrates to aragonite on the order of minutes to hours [9], detected vaterite in the predominantly aragonite skeleton has been proposed as a precursor mineral [16], and an Antarctic stony coral presents a high-Mg-calcite inner skeleton surrounded by a thicker aragonitic outer skeleton [17]. Among the octocorals, soft corals produce a wide variety of minerals including Mg-calcite sclerites [18] and Mg-calcite, aragonite, and amorphous calcium cementing materials [5]. That these findings of polymineralogy are recent suggests that there is likely more variability in the mineral composition within the calcifying anthozoans than previously realized.

The various calcium carbonate polymorphs, whether produced by organisms or abiotically, display a range of thermodynamic stabilities under natural conditions [e.g., 19]. In contrast to calcite - the most stable calcium carbonate polymorph - and aragonite which both can persist unaltered for hundreds of millions of years in the fossil record [e.g., 20, 21], vaterite is highly unstable at ambient conditions and is more soluble than calcite or aragonite [22, 23], although it has been observed to naturally precipitate inorganically under extreme conditions (e.g., cold, dry, and highly alkaline [24]) and is more stable than amorphous calcium carbonate. Biological vaterite deposits tend to have a spherical shape with a porous inner structure, can have a rough outer surface, and range in size from 0.05 to 5 μm [25, 26]. Abiotically, it can precipitate in solutions with relatively high pHs of from 8.5 to 9.9 [27, 28]. Once exposed to distilled water or water containing salts, vaterite transforms to calcite (elevated temperature) or aragonite (ambient and elevated temperatures) [29 and references therein, 30]. It is therefore found in nature in relatively small amounts and often as part of a mixture of different phases [e.g., 31, 32]. Despite its metastability, so far vaterite has been identified in various biominerals such as fish otoliths, freshwater pearls, healed scars of some mollusk shells, gallstones, ascidians, and terrestrial plants, and associated with microbial mats among others [33–38].

Members of the octocoral family Xeniidae form a major component of shallow coral-reef communities in the tropical Indo-West-Pacific region [39]. In the Red Sea in particular, a remarkably high number of species of this family have been recorded [e.g., 40, 41], many of which were originally described there, and some are considered to be endemic to the region [41]. The xeniids form, for the most part, small and soft colonies, which are often slippery due to their secretion of large amounts of mucus [42]. Previous investigations indicate that they are ephemeral pioneer organisms, with rapid growth rates, high fecundity, and extensive vegetative reproductive capabilities [43]. Ecologically, they are important early colonizers of reefs after major disturbance and consequently take over degraded reef substrata [e.g., 44, 45]. For instance, following crown of thorns starfish outbreaks, cyclones, and coral

bleaching on the Great Barrier Reef (Australia), increased soft coral abundance was noted with Xeniidae as the most common family (http://www.aims.gov.au/index.html). Similarly, reef deterioration in Sabah (East Malaysia) was associated with increased abundance of xeniids, which act there as barriers to recruitment of stony corals [46]. It is evident, therefore, that Xeniidae have become highly relevant to tropical and sub-tropical shallow reef ecology.

Despite being the second most abundant benthic group of organisms on coral reefs, octocorals are not usually considered as reef-builders, although a few taxa do produce massive aragonite skeletons [e.g., 42, 47]. Instead, octocorals feature a high density of internal calcium carbonate sclerites in all parts of the colony [e.g., 40, 41, 42]. Studies have shown the significance of the integration of classical taxonomy, including sclerite morphology, along with molecular phylogenetic analyses in order to delineate species boundaries [e.g., 48, 49, 50]. The sclerites of a number of xeniid genera are relatively simple, being shaped as small round platelets or spheroids with a smooth surface as observed by light microscopy [42]. Scanning electron microscopy (SEM) has further revealed microstructural features of sclerites of some xeniids in which their surfaces are actually formed of corpuscular aggregations of microscleres, the first such observations among octocorals [39, 51]. In fact, the taxonomic establishment of the genus *Ovabunda* was based on this microstructural novelty and later genetically confirmed [52, 53]. This genus is now known to be highly abundant in the Gulf of Aqaba (northern Red Sea) with *O. macrospiculata* (formerly named *Xenia macrospiculata*) being the most common species there [40, 48, 54, 55].

Because *O. macrospiculata* is such an abundant and ecologically important benthic inhabitant in Red Sea coral reefs and it displays an interesting apparent microsclere surface composition of its sclerites, we carefully examined its sclerites by multiple techniques to more firmly establish their elemental content and mineralogy. Here, we show by SEM, Raman spectroscopy, and X-ray diffraction that *O. macrospiculata* sclerites are composed primarily of vaterite. This has implications for the persistence of *O. macrospiculata* and its ability to continue to form what is typically considered to be a metastable calcium carbonate in the face of ocean acidification, as well as for the presence of this calcium carbonate polymorph in other related taxa. It is also a crucial first step in establishing if the function of vaterite sclerites differs from that of the more commonly detected calcite sclerites.

2 Materials and methods

2.1 Sample collection

O. macrospiculata, a branching soft coral with multiple polyps at the ends of each branch, is capable of both branch fission and subsequent colony migration, yielding colonies of varying sizes and ages [43 and references therein]. Colonies of *O. macrospiculata* were collected under a permit issued by the Israel Nature and Parks Authority from the reef adjacent to the Interuniversity Institute for Marine Sciences (Eilat, northern Gulf of Aqaba) at depths of 5-6 m (July 2016) and preserved in 70% ethanol. Polyps were removed from the colonies, placed in separate Eppendorf tubes, and 10% sodium hypochlorite was added to dissolve the tissues. After 20–30 min, the supernatant and organic debris were discarded and

the sclerites were carefully and gently rinsed 4–5 times in distilled water to remove excess bleach and debris [39]. Following all analyses described below, the sclerites were deposited in the Steinhardt Museum of Natural History at Tel Aviv University under catalog number SMNHTAU Co 36488 (https://smnh.tau.ac.il/en/research/collections-database/, registration required for access).

2.2 SEM with EDS and sample preparation

A subsample of washed sclerites resuspended in 100% ethanol was pipetted onto a silicon wafer, allowed to dry, and coated in gold. The sclerites were examined using a scanning electron microscope (ZEISS SigmaTM SEM Germany) coupled with energy-dispersive X-ray spectrometry (EDS, Quantax, Bruker), with an in-lens detector (2 kV, WD = 3.5–5 mm). Elemental analyses by EDS were performed in locations of interest that were chosen after secondary electron imaging in the SEM (20 kV, WD = 7-8 mm). Two to four replicate regions of interest on five sclerites were spot-analyzed for element quantification, with 20 second live times. Several other sclerites were analyzed for whole-sclerite element mapping with live times of 49 seconds each. Elemental relative abundance quantification and element distribution map production were conducted using AZtec software (Oxford Instruments).

2.3 Raman measurements on isolated and *in vivo* sclerites

Raman is a non-destructive inelastic spectroscopy which produces vibrational spectra to unequivocally identify minerals and their polymorphs. All Raman measurements were carried out using a Horiba (France) LabRAM HR Evolution instrument equipped with four laser lines (325 nm, 532 nm, 633 nm, and 785 nm). We use several excitation lines to avoid fluorescence and obtain the highest signal to noise ratio possible. It is also possible to choose a diffraction grating in order to achieve a suitable spectral resolution with the 800 mm focal length of the spectrograph. The instrument uses a modular microscope Olympus BX-FM and we chose a suitable objective for each sample and analysis type as described below. Signals were detected by an open electrode, front illuminated, cooled CCD detector Horiba Syncerity (USA), and signal intensity at each wavenumber step was normalized to the highest measured intensity of each measured spectrum for graphing purposes. As the spot size of the laser beam under the objective is smaller than 1 micrometer it is hard to determine all components of a heterogenous system and minor compounds may not be detected unless long measurement schemes are utilized. Therefore, it is reasonable to assume that not all minor components of the corals were detected by Raman.

2.3.1 In-vitro Raman and sample preparation—Isolated sclerites were resuspended in 100% ethanol. A subsample was then pipetted onto a glass slide and left to dry; no sea salt was observed crystallized on the prepared slides. The samples were measured with a 0.9 numerical aperture MPlanFL N 100x objective (Olympus) in ambient air.

2.3.2 In-vivo Raman and sample preparation—A colony of *O. macrospiculata* was transferred from Eilat, alive in seawater, to the Weizmann Institute in Rehovot, Israel without any pretreatment. One polyp was excised from the colony and measurements were conducted on various places along the stem of its body with a water immersion 1.0 numerical aperture LUMPlanFL N 60x objective (Olympus) in the original seawater in

which the colony was collected, as described previously by [56], without anesthetization by $MgCl_2$ addition. Initially, spot analyses were conducted on the polyp so as to stress the animal as little as possible. Spot measurements were repeated after 24 hours on the same colony, including on tissue locations in which no sclerites were observed in order to determine the background signal. At that time, we also conducted an *in-vivo* Raman mapping of mineral distribution. Map pixels were smoothed in ImageJ.

2.4 High-resolution synchrotron powder X-ray diffraction

High-resolution powder X-ray diffraction (HRPXRD) was performed on isolated sclerites using synchrotron radiation (wavelength 0.457890Å) at the 11-BM-B beamline of the Advanced Photon Source, Argonne National Laboratory, USA. The samples were loaded into 0.9-mm glass capillaries and scanned while being rotated. The Rietveld refinement method in GSAS-II software was used for data analysis and also allowed for relative quantification of all polymorphs present [57].

3 Results

After isolating the sclerites from several *O. macrospiculata* polyps (Figure 1A), we examined them by SEM. Aggregates of sclerites (Figure 1B) were observed at higher magnifications to be composed of smaller rounded corpuscular-shaped microscleres 0.5-1 μm in diameter with a nanogranular surface pattern (Figure 1C, D). EDS analysis finds abundant magnesium and calcium both by spot analyses (Figure 1E, F) as well as across the entirety of the aggregate (Figure 1G–J, same location as B, Table S1). The abundance of magnesium was confirmed in other sclerite aggregates as well (e.g., Figure S1).

In-vitro micro-Raman spectroscopy of isolated sclerites shows peak positions characteristic of vaterite (120 cm^{-1}, 206 cm^{-1}, 265 cm^{-1}, 300 cm^{-1}, 739 cm^{-1}, 749 cm^{-1}, a main peak at 1090cm^{-1} with a shoulder at 1071cm^{-1} [58, 59] (Figure 2A, black line). *In-vivo* Raman yielded the above peaks for vaterite as well as for aragonite (155 cm^{-1}, 205 cm^{-1}, 701 cm^{-1}, 704 cm^{-1}, 1437 cm^{-1} and the main peak at 1086 cm^{-1}, out of the 30 active Raman modes) [60] (Figure 2A, red line). To confirm that the presence of vaterite, the least stable of the non-hydrated calcium carbonate common biogenic polymorphs, did not result from the isolated sclerite preparation process, we analyzed sclerites in living xeniid tissue by *in-vivo* micro-Raman spectroscopy. This analysis showed the presence of both vaterite and aragonite in sclerite aggregates (Figure 2A, red and green lines, respectively). The measurement of the Raman spectra of the sclerites was repeated *in-vivo* one day later to verify that the presence of vaterite in the living tissue, although the major component of the sclerites, did not dramatically decline as vaterite is normally considered to be a metastable polymorph. Both spot analysis and mapping across two polyps confirmed that the vaterite in the sclerites remained after 24 hours, as did aragonite (Figure 2B, red line; 2C-E). It should be noted that the positions of both the lattice-mode peak and that of the carbonate ion v_1 mode (symmetric stretching mode) of the *in-vivo* Raman analysis are shifted to higher wavenumbers as compared to that of pure vaterite; it has been shown that incorporation of magnesium into the lattice of Mg-calcium carbonates, and specifically vaterite, can cause such a shift [61, 62]. There is also a good correlation between the amount of magnesium

detected via EDS and the corresponding shift in wavenumber (η_{Mg} = Mg/(Ca + Mg) ~ 6.4 atom %, Table S1).

To quantify mineralogical fractions, as well as to estimate the amount of incorporated magnesium in the vaterite lattice, we conducted high-resolution synchrotron X-ray powder diffraction (HRPXRD) on isolated sclerites. Following Reitveld analysis, we could determine that vaterite appears to be the major mineral phase at 98-99%, with much smaller amounts of calcite and aragonite (Figure 3). Because diffraction was acquired from the whole volume of the isolated sclerites and due to the low detection limit of synchrotron X-rays, the calcite phase could be identified in the composition of the sclerites even though its fraction was as low as ~1 wt. %, as could the similarly low-abundance aragonite which was detected by micro-Raman. We also note several diffraction peaks that match the dominant reflections of sodium chloride; this most likely could be due to the cleaning solution, sodium hypochlorite, used to dissolve organic tissues around the sclerites, remaining between microsclerites that was not removed during the rinsing process. In order to calculate the amount of magnesium in the vaterite lattice based on the diffraction data we obtained the lattice parameters from the Reitveld analysis: a = 4.0985 ± 3 Å, c = 8.4120 ± 2 Å. Comparing this data to that of [61] we find that these lattice parameters correspond to a range of 4.4 atom % Mg (based on the a lattice parameter), a value quite close to the 6.4 atom % determined by EDS as noted above.

4 Discussion

Cnidarian calcium carbonate hard components, such as external skeletons and internal sclerites, serve important functions, from protecting against predation to supporting mechanics of colony movement to scattering light for enhanced photosynthesis by endosymbionts [e.g., 63, 64, 65]. Cnidarians produce predominantly aragonitic or calcitic hard structures within or outside their tissues, which has been well-documented across a variety of taxa [reviewed by 66]. Here, we report for the first time, the occurrence of vaterite in soft coral sclerites.

In biomineralization there are few known occurrences of biogenic vaterite. It has historically been observed as a minor component of a larger hard structure, suggested as a precursor phase for a more stable form of calcium carbonate [e.g., 16], or as the result of a defective biological process. Some examples can be found in green turtle eggshells [67], coho salmon otoliths [59], freshwater lackluster pearls [68], and the abnormal growth of mollusk shells repaired after fracture [69]. It can also result from induced mineralization, i.e., as an unintended biproduct of biological processes [1], such as vaterite precipitation by soil bacteria leading to their encapsulation and fossilization [26]. A rare and unique example where vaterite is deposited as the only mineral component of an organism's endoskeleton and clearly as the result of controlled biomineralization, where production of the mineral occurs in a delineated space containing a preformed and purposeful organic matrix [1], is the body and tunic spicules of the ascidian *Herdmania momus* [35, 70, 71]. In snails, its presence in egg capsules may serve as a calcium store benefited by its metastability [72]. Within Cnidaria, vaterite has been suggested as an aragonite precursor in stony corals [16], although high-resolution analysis has found that coral skeleton is >99% aragonite [73]. As

vaterite is not the most stable form of biogenic calcium carbonate mineral it may serve as a metastable precursor for a more stable polymorph, or have a specific role fitting its chemical and mechanical properties. Another option which should be examined is whether it is the product of a less stable precursor such as amorphous calcium carbonate (ACC).

The nanogranular surface of *O. macrospiculata* microscleres is suggestive of formation by particle attachment [74]. This has been observed in newly formed aragonite of stony corals that results from a particle-by-particle process that uses amorphous calcium carbonate, which like vaterite also exhibits low stability, as the mineral precursor [9]. Biogenic vaterite formation via particle attachment has also been observed in tunicate spicules [75]. Inorganic precipitation experiments have shown that microcrystals of vaterite aggregate in an oriented process to yield products with a granular surface at the sub-micron scale [76]. However, vaterite formation by living organisms is not simply an inorganic process. The highly acidic stony coral skeletal protein, coral acid rich protein 3 (CARP3) as well as extracted stony coral skeletal organic matrix protein complexes, can direct calcium carbonate formation toward vaterite *in-vitro* [77, 78]. Differing peptides have been detected in vaterite versus aragonite in mussel shells and fish otoconia [79, 80], which could further reinforce the nanocrystalline appearance of the mineral surface as has been observed in stony corals [81, 82]. Further, bacterially-mediated formation of vaterite also yields oriented nanocrystals within the spheroids [26]. Additionally, the presence of organic matter [reviewed by 83] or high concentrations of phosphate [37] can serve to stabilize vaterite and prevent its transformation to calcite or aragonite. While the organic matter composition and chemistry of the calcifying precursor solution of the *O. macrospiculata* sclerites is currently unknown, there appears to be a core set of sclerite proteins conserved across other soft coral taxa, including scleritin, carbonic anhydrase, and acidic proteins [84].

Anthropogenic increases in atmospheric pCO_2 lead to ocean acidification, which may be detrimental to calcifying marine organisms [10]. Production of what is typically considered a less-stable polymorph of calcium carbonate could therefore prove problematic for soft corals that deposit vaterite sclerites. However, no difference was observed in the ratio of sclerite to polyp tissue mass or sclerite microstructure for *O. macrospiculata* reared under increased pCO_2 conditions, suggesting that the animal tissue provides protection from the possible negative effects of lower pH [14, 85], despite what we now show to be a $CaCO_3$ polymorph, typically considered to be metastable, comprising the sclerites. That the vaterite of the sclerites did not recrystallize over a 24-hour period suggests that, in the living tissue, it is not, in fact, metastable. This has profound implications for our understanding of how xeniid taxa, which can rapidly colonize newly available reef substrate [44], will interact with the more prominent reef-building corals [43, 86], whose skeleton is external, as reef-building corals face anthropogenic climate change including ocean acidification. Further, as the present work is the first description of vaterite in soft coral sclerites, it is currently unknown if production and maintenance of this vaterite has changed in recent years as the corals have experienced increased acidified ocean conditions due to increased input of anthropogenic CO_2 [87] or faster warming of the surface ocean in the Red Sea compared to the global average [88]. A recent study in juvenile sturgeon showed that otoliths of fish reared at either increased pCO_2 or increased pCO_2 plus increased temperature did not exhibit significant

decreases in the abundance of vaterite [89], an observation previously reported for increased pCO_2 for other fish taxa [e.g., 90].

It is not easy to clearly conclude whether the vaterite in this system is formed via biologically induced versus biologically controlled biomineralization; however, the observation by HRPXRD that ~99 wt.% of the mineral is vaterite combined with the observations that the microscleres aggregate and demonstrate uniform sizes and architecture and are maintained for at least 24 hours *in vivo* are a strong indication that they were formed via a process controlled by the animal. This is a significant finding as, if indeed *O. macrospiculata* sclerites are formed via controlled biomineralization, it is only the second report of controlled biomineralization of vaterite with the first being from tunicates [35]. Moreover, the presence of significant amounts of magnesium in *O. macrospiculata* sclerites (Figure 1F, Table S1, Reitveld calculations), as well as Raman peak shifting to higher wavenumbers (Table S2) and symmetric stretching (Figure 3) strengthens the hypothesis that crystallization occurred via an amorphous precursor as previously reported for bioinspired synthetic vaterite shown to incorporate in its structure magnesium ions when crystallized via an amorphous precursor [61]. In the present species, this vaterite then appears stable as it persists as the predominant polymorph. Differential charges on molecules of a biochemical component of the sclerites, potentially including proteins similar to those recently sequenced from several octocoral species [91], could serve in nucleating and stabilizing initial nanoparticles of vaterite as proposed by [92].

5 Conclusions

Soft coral sclerites from various taxa have previously been reported as calcite with some cementing material as aragonite. Here we show that both preserved and *in-vivo* sclerites of *O. macrospiculata* are composed primarily of vaterite with a smaller fraction of aragonite and calcite. While their function and the biological mechanism underpinning their formation in the tissue remain to be studied, determining this novel mineralogy in this ecologically important octocoral is a crucial first step and we anticipate that it will be found in other soft coral taxa as well.

Supplementary Material

Refer to Web version on PubMed Central for supplementary material.

Acknowledgements

We thank Alex Shlagman at the Steinhardt Museum of Natural History at Tel Aviv University for curatorial skills, Ronen Liberman at Tel Aviv University for the underwater photograph of the live *O. macrospiculata* and for collecting live specimens for *in-vivo* Raman spectroscopy, Marcus Lin at the University of California Los Angeles for technical assistance, and the staff of the Interuniversity Institute for Marine Science in Eilat (IUI) for their hospitality and use of facilities. BP and IPo acknowledge the use of the 11-BM-B beamline of the Advanced Photon Source, Argonne National Laboratory, USA. IPi is the incumbent of the Sharon Zuckerman Research Fellow Chair. We thank the two anonymous reviewers for helpful comments.

Europe PMC Funders Author Manuscripts

7 Funding

JLD was supported by the Zuckerman STEM Leadership Program. This work has received funding to TM from the European Research Council under the European Union's Horizon 2020 research and innovation programme (grant agreement No 755876).

References

[1]. Lowenstam, HA, Weiner, S. On Biomineralization. Oxford University Press, New York; New York: 1989.

[2]. Cairns SD, Macintyre IG. Phylogenetic implications of calcium carbonate mineralogy in the Stylasteridae (Cnidaria: Hydrozoa). Palaios. 1992 :96–107.

[3]. Zhang F, Cai W, Zhu J, Sun Z, Zhang J. In situ raman spectral mapping study on the microscale fibers in blue coral (*Heliopora coerulea*) skeletons. Analytical Chemistry. 2011; 83 (20) :7870–7875. [PubMed: 21882838]

[4]. Drake J, Mass T, Stolarski J, Von Euw S, van de Schootbrugge B, Falkowski PG. How corals made rocks through the ages. Global Change Biol. 2020; 26 (1) :31.

[5]. Shoham E, Prohaska T, Barkay Z, Zitek A, Benayahu Y. Soft corals form aragonite-precipitated columnar spiculite in mesophotic reefs. Scientific Reports. 2019; 9 (1) :1–9. [PubMed: 30626917]

[6]. Weinbauer MG, Vellmirov B. Calcium, magnesium and strontium concentrations in the calcite sclerites of Mediterranean gorgonians (Coelenterata: Octocorallia). Estuarine, Coastal and Shelf Science. 1995; 40 (1) :87–104.

[7]. Dunkelberger DG, Watabe N. An ultrastructural study on spicule formation in the pennatulid colony *Renilla reniformis* . Tissue and Cell. 1974; 6 (4) :573–586. [PubMed: 4156429]

[8]. Vielzeuf D, Gagnon AC, Ricolleau A, Devidal J-L, Balme-Heuze C, Yahiaoui N, Fonquernie C, Perrin J, Garrabou J, Montel J-M. Growth kinetics and distribution of trace elements in precious corals. Frontiers in Earth Science. 2018; 6 :167.

[9]. Mass T, Giuffre AJ, Sun C-Y, Stifler CA, Frazier MJ, Neder M, Tamura N, Stan CV, Marcus MA, Gilbert PUPA. Amorphous calcium carbonate particles from coral skeletons. Proceedings of the National Academy of Sciences. 2017; 114 (37) :E7670–E7678.

[10]. Doney SC, Busch DS, Cooley SR, Kroeker KJ. The impacts of ocean acidification on marine ecosystems and reliant human communities. Annual Review of Environment and Resources. 2020; 45 :83–112.

[11]. Comeau S, Edmunds PJ, Spindel NB, Carpenter RC. The responses of eight coral reef calcifiers to increasing partial pressure of CO_2 do not exhibit a tipping point. Limnol Oceanogr. 2013; 58 (1) :388–398.

[12]. Gómez CE, Paul VJ, Ritson-Williams R, Muehllehner N, Langdon C, Sánchez JA. Responses of the tropical gorgonian coral *Eunicea fusca* to ocean acidification conditions. Coral Reefs. 2014 :1–10.

[13]. Bramanti L, Movilla J, Guron M, Calvo E, Gori A, Dominguez-Carrió C, Grinyó J, Lopez-Sanz A, Martinez-Quintana A, Pelejero C. Detrimental effects of ocean acidification on the economically important Mediterranean red coral (*Corallium rubrum*). Global Change Biol. 2013; 19 (6) :1897–1908.

[14]. Gabay Y, Benayahu Y, Fine M. Does elevated pCO_2 affect reef octocorals? Ecology and Evolution. 2013; 3 (3) :465–473. [PubMed: 23533159]

[15]. McFadden CS, Quattrini AM, Brugler MR, Cowman PF, Dueñas LF, Kitahara MV, Paz-García DA, Reimer JD, Rodríguez E. Phylogenomics, origin, and diversification of anthozoans (phylum Cnidaria). Syst Biol. 2021

[16]. Song Y, Yu K, Ayoko GA, Frost RL, Shi Q, Feng Y, Zhao J. Vibrational spectroscopic characterization of growth bands in *Porites* coral from South China Sea. Spectrochimica Acta Part A: Molecular and Biomolecular Spectroscopy. 2013; 112 :95–100.

[17]. Stolarski J, Coronado I, Murphy JG, Kitahara MV, Janiszewska K, Mazur M, Gothmann AM, Bouvier A-S, Marin-Carbonne J, Taylor ML. A modern scleractinian coral with a two-component calcite-aragonite skeleton. Proceedings of the National Academy of Sciences. 2021; 118 (3)

[18]. Rahman MA, Oomori T. Structure, crystallization and mineral composition of sclerites in the alcyonarian coral. Journal of Crystal Growth. 2008; 310 (15) :3528–3534.

[19]. Sekkal W, Zaoui A. Nanoscale analysis of the morphology and surface stability of calcium carbonate polymorphs. Scientific Reports. 2013; 3 (1) :1–10.

[20]. Gothmann AM, Stolarski J, Adkins JF, Schoene B, Dennis KJ, Schrag DP, Mazur M, Bender ML. Fossil corals as an archive of secular variations in seawater chemistry since the Mesozoic. Geochim Cosmochim Acta. 2015; 160 (0) :188–208.

[21]. Janiszewska K, Mazur M, Machalski M, Stolarski J. From pristine aragonite to blocky calcite: Exceptional preservation and diagenesis of cephalopod nacre in porous Cretaceous limestones. PLoS ONE. 2018; 13 (12) e0208598 [PubMed: 30566495]

[22]. Plummer LN, Busenberg E. The solubilities of calcite, aragonite and vaterite in CO_2-H_2O solutions between 0 and 90 C, and an evaluation of the aqueous model for the system $CaCO_3$-CO_2-H_2O. Geochim Cosmochim Acta. 1982; 46 (6) :1011–1040.

[23]. Ogino T, Suzuki T, Sawada K. The formation and transformation mechanism of calcium carbonate in water. Geochim Cosmochim Acta. 1987; 51 (10) :2757–2767.

[24]. Grasby SE. Naturally precipitating vaterite (μ-$CaCO_3$) spheres: unusual carbonates formed in an extreme environment. Geochim Cosmochim Acta. 2003; 67 (9) :1659–1666.

[25]. Yamamoto H, Sakae T, Schäfer H. Analysis of vaterite microspherolith deposits on a pure cholesterol gallstone by X-ray diffraction, X-ray microanalysis and infrared absorption techniques. Virchows Archiv A. 1985; 405 (4) :463–471.

[26]. Rodriguez-Navarro C, Jimenez-Lopez C, Rodriguez-Navarro A, Gonzalez-Muñoz MT, Rodriguez-Gallego M. Bacterially mediated mineralization of vaterite. Geochim Cosmochim Acta. 2007; 71 (5) :1197–1213.

[27]. Kralj D, Brecevic L, Nielsen AE. Vaterite growth and dissolution in aqueous solution I. Kinetics of crystal growth. Journal of Crystal Growth. 1990; 104 (4) :793–800.

[28]. Vecht A, Ireland T. The role of vaterite and aragonite in the formation of pseudo-biogenic carbonate structures: Implications for Martian exobiology. Geochim Cosmochim Acta. 2000; 64 (15) :2719–2725. [PubMed: 11543352]

[29]. Johnston J. The several forms of calcium carbonate. Am J Sci. 1916; 4 (246) :473–512.

[30]. Bischoff J. Catalysis, inhibition, and the calcite-aragonite problem;[Part] 2, The vateritearagonite transformation. Am J Sci. 1968; 266 (2) :80–90.

[31]. Soldati A, Jacob D, Wehrmeister U, Hofmeister W. Structural characterization and chemical composition of aragonite and vaterite in freshwater cultured pearls. Mineralogical Magazine. 2008; 72 (2) :579–592.

[32]. Nehrke G, Poigner H, Wilhelms-Dick D, Brey T, Abele D. Coexistence of three calcium carbonate polymorphs in the shell of the Antarctic clam *Laternula elliptica* . Geochemistry, Geophysics, Geosystems. 2012; 13 (5)

[33]. Prien EL, Frondel C. Studies in urolithiasis: I. The composition of urinary calculi. The Journal of Urology. 1947; 57 (6) :949–991. [PubMed: 20243909]

[34]. Hall A, Taylor J. The occurrence of vaterite in gastropod egg-shells. Mineralogical Magazine. 1971; 38 (296) :521–522.

[35]. Lowenstam HA, Abbott DP. Vaterite: A mineralization product of the hard tissues of a marine organism (Ascidiacea). Science. 1975; 188 (4186) :363–365. [PubMed: 1118730]

[36]. Rodgers AL. Common ultrastructural features in human calculi. Micron and Microscopica Acta. 1983; 14 (3) :219–224.

[37]. Giralt S, Julià R, Klerkx J. Microbial biscuits of vaterite in lake Issyk-Kul (Republic of Kyrgyzstan). Journal of Sedimentary Research. 2001; 71 (3) :430–435.

[38]. David AW, Grimes CB, Isely JJ. Vaterite sagittal otoliths in hatchery-reared juvenile red drums. The Progressive Fish-Culturist. 1994; 56 (4) :301–303.

[39]. Aharonovich D, Benayahu Y. Microstructure of octocoral sclerites for diagnosis of taxonomic features. Mar Biodiv. 2012; 42 (2) :173–177.

[40]. Halász A, McFadden CS, Aharonovich D, Toonen R, Benayahu Y. A revision of the octocoral genus *Ovabunda*, Alderslade, 2001 (Anthozoa, Octocorallia, Xeniidae). ZooKeys. 2014; (373) :1.

[41]. Halász A, McFadden CS, Toonen R, Benayahu Y. Re-description of type material of *Xenia*, Lamarck, 1816 (Octocorallia: Xeniidae). Zootaxa. 2019; 4652 (2) zootaxa. 4652.2. 1-zootaxa. 4652.2. 1

[42]. Fabricius, K, Alderslade, P. Soft corals and sea fans: A comprehensive guide to the tropical shallow water genera of the central-west Pacific, the Indian Ocean and the Red Sea. Australian Institute of Marine Science; 2001.

[43]. Benayahu Y, Loya Y. Settlement and recruitment of a soft coral: Why is *Xenia macrospiculata* a successful colonizer? Bull Mar Sci. 1985; 36 (1) :177–188.

[44]. Reinicke, GB. Contributions to systematics and ecology. Burghard, W, Kuttler, W, Schuhmacher, H, editors. Essener Ökologische Schriften; 1995. 193

[45]. Tilot V, Leujak W, Ormond R, Ashworth J, Mabrouk A. Monitoring of South Sinai coral reefs: Influence of natural and anthropogenic factors. Aquat Conserv: Mar Freshwat Ecosyst. 2008; 18 (7) :1109–1126.

[46]. Wood, E; Dipper, F. What is the future for extensive areas of reef impacted by fish blasting and coral bleaching and now dominated by soft corals? A case study from Malaysia; Proceedings of the 11th International Coral Reef Symposium; Fort Lauderdale (USA). 2008. 410–414.

[47]. Miyazaki Y, Reimer JD. A new genus and species of octocoral with aragonite calciumcarbonate skeleton (Octocorallia, Helioporacea) from Okinawa, Japan. ZooKeys. 2015; (511) :1.

[48]. Halász A, Reynolds AM, McFadden CS, Toonen RJ, Benayahu Y. Could polyp pulsation be the key to species boundaries in the genus *Ovabunda* (Octocorallia: Alcyonacea: Xeniidae)? Hydrobiologia. 2015; 759 (1) :95–107.

[49]. Benayahu Y, van Ofwegen LP, McFadden CS. Evaluating the genus *Cespitularia*, MilneEdwards & Haime, 1850 with descriptions of new genera of the family Xeniidae (Octocorallia, Alcyonacea). ZooKeys. 2018; (754) :63.

[50]. Stemmer K, Burghardt I, Mayer C, Reinicke GB, Wägele H, Tollrian R, Leese F. Morphological and genetic analyses of xeniid soft coral diversity (Octocorallia; Alcyonacea). Organisms Diversity & Evolution. 2013; 13 (2) :135–150.

[51]. Benayahu Y. Xeniidae (Cnidaria: Octocorallia) from the Red Sea, with the description of a new species. Zoologische Mededelingen. 1990; 64 (9) :113–120.

[52]. Alderslade P. Six new genera and six new species of soft corals, and some proposed familial and subfamilial changes within the Alcyonaea (Coelonterata: Octocorallia. Bull Biol Soc Wash. 2001; 10 :15–65.

[53]. McFadden CS, Haverkort-Yeh R, Reynolds AM, Halàsz A, Quattrini AM, Forsman ZH, Benayahu Y, Toonen RJ. Species boundaries in the absence of morphological, ecological or geographical differentiation in the Red Sea octocoral genus *Ovabunda* (Alcyonacea: Xeniidae). Mol Phylogen Evol. 2017; 112 :174–184.

[54]. Benayahu Y, Loya Y. Life history studies on the Red Sea soft coral *Xenia macrospiculata* Gohar, 1940. I. Annual dynamics of gonadal development. The Biological Bulletin. 1984; 166 (1) :32–43.

[55]. Benayahu Y, Loya Y. Life history studies on the Red Sea soft coral *Xenia macrospiculata* Gohar, 1940. II. Planulae shedding and post larval development. The Biological Bulletin. 1984; 166 (1) :44–53.

[56]. Akiva A, Neder M, Kahil K, Gavriel R, Pinkas I, Goobes G, Mass T. Minerals in the pre-settled coral *Stylophora pistillata* crystallize via protein and ion changes. Nature Communications. 2018; 9 (1) 1880

[57]. Toby BH, Von Dreele RB. GSAS-II: The genesis of a modern open-source all purpose crystallography software package. Journal of Applied Crystallography. 2013; 46 (2) :544–549.

[58]. Donnelly F, Purcell-Milton F, Framont V, Cleary O, Dunne P, Gun'ko Y. Synthesis of $CaCO_3$ nano-and micro-particles by dry ice carbonation. Chemical Communications. 2017; 53 (49) :6657–6660. [PubMed: 28585625]

[59]. Wehrmeister U, Soldati AL, Jacob D, Häger T, Hofmeister W. Raman spectroscopy of synthetic, geological and biological vaterite: A Raman spectroscopic study. Journal of Raman Spectroscopy: An International Journal for Original Work in all Aspects of Raman Spectroscopy,

Including Higher Order Processes, and also Brillouin and Rayleigh Scattering. 2010; 41 (2) :193–201.

[60]. De La Pierre M, Carteret C, Maschio L, André E, Orlando R, Dovesi R. The Raman spectrum of $CaCO_3$ polymorphs calcite and aragonite: A combined experimental and computational study. The Journal of Chemical Physics. 2014; 140 (16) 164509 [PubMed: 24784289]

[61]. Seknazi E, Mijowska S, Polishchuk I, Pokroy B. Incorporation of organic and inorganic impurities into the lattice of metastable vaterite. Inorganic Chemistry Frontiers. 2019; 6 (10) :2696–2703.

[62]. Bischoff WD, Sharma SK, MacKenzie FT. Carbonate ion disorder in synthetic and biogenic magnesian calcites: a Raman spectral study. American Mineralogist. 1985; 70 (5–6) :581–589.

[63]. Clavico EE, De Souza AT, Da Gama BA, Pereira RC. Antipredator defense and phenotypic plasticity of sclerites from *Renilla muelleri* a tropical sea pansy. The Biological Bulletin. 2007; 213 (2) :135–140. [PubMed: 17928520]

[64]. Lewis J, Wallis E. The function of surface sclerites in gorgonians (Coelenterata, Octocorallia). The Biological Bulletin. 1991; 181 (2) :275–288. [PubMed: 29304649]

[65]. Enríquez S, Méndez ER, Iglesias-Prieto R. Multiple scattering on coral skeletons enhances light absorption by symbiotic algae. Limnol Oceanogr. 2005; 50 (4) :1025–1032.

[66]. Cuif, J-P. The Cnidaria, Past, Present and Future. Goffredo, S, Dubinsky, Z, editors. Springer; 2016. 875

[67]. Lakshminarayanan R, Chi-Jin EO, Loh XJ, Kini RM, Valiyaveettil S. Purification and characterization of a vaterite-inducing peptide, pelovaterin, from the eggshells of *Pelodiscus sinensis* (Chinese soft-shelled turtle). Biomacromolecules. 2005; 6 (3) :1429–1437. [PubMed: 15877362]

[68]. Qiao L, Feng Q. Study on twin stacking faults in vaterite tablets of freshwater lacklustre pearls. Journal of Crystal Growth. 2007; 304 (1) :253–256.

[69]. Spann N, Harper EM, Aldridge DC. The unusual mineral vaterite in shells of the freshwater bivalve *Corbicula fluminea* from the UK. Naturwissenschaften. 2010; 97 (8) :743–751. [PubMed: 20567799]

[70]. Kabalah-Amitai L, Mayzel B, Zaslansky P, Kauffmann Y, Clotens P, Pokroy B. Unique crystallographic pattern in the macro to atomic structure of *Herdmania momus* vateritic spicules. Journal of Structural Biology. 2013; 183 (2) :191–198. [PubMed: 23669626]

[71]. Kabalah-Amitai L, Mayzel B, Kauffmann Y, Fitch AN, Bloch L, Gilbert PU, Pokroy B. Vaterite crystals contain two interspersed crystal structures. Science. 2013; 340 (6131) :454–457. [PubMed: 23620047]

[72]. Meenakshi V, Blackwelder P, Watabe N. Studies on the formation of calcified egg-capsules of ampullarid snails. Calcif Tissue Res. 1974; 16 (1) :283–291. [PubMed: 4451868]

[73]. Von Euw S, Zhang Q, Manichev V, Murali N, Gross J, Feldman LC, Gustafsson T, Flach C, Mendelsohn R, Falkowski PG. Biological control of aragonite formation in stony corals. Science. 2017; 356 (6341) :933–938. [PubMed: 28572387]

[74]. De Yoreo JJ, Gilbert PUPA, Sommerdijk NAJM, Penn RL, Whitelam S, Joester D, Zhang H, Rimer JD, Navrotsky A, Banfield JF, Wallace AF, et al. Crystallization by particle attachment in synthetic, biogenic, and geologic environments. Science. 2015; 349 (6247) aaa6760-aaa6760 [PubMed: 26228157]

[75]. Gilbert PU, Porter SM, Sun C-Y, Xiao S, Gibson BM, Shenkar N, Knoll AH. Biomineralization by particle attachment in early animals. Proceedings of the National Academy of Sciences. 2019; 116 (36) :17659–17665.

[76]. Zhou G-T, Yao Q-Z, Fu S-Q, Guan Y-B. Controlled crystallization of unstable vaterite with distinct morphologies and their polymorphic transition to stable calcite. European Journal of Mineralogy. 2010; 22 (2) :259–269.

[77]. Laipnik, Ra; Bissi, V; Sun, C-Y; Falini, G; Gilbert, PU; Mass, T. Coral acid rich protein selects vaterite polymorph in vitro. Journal of Structural Biology. 2020; 209 (2) 107431 [PubMed: 31811894]

[78]. Hohn S, Reymond CE. Coral calcification, mucus, and the origin of skeletal organic molecules. Coral Reefs. 2019; 38 :973–984.

[79]. Berland S, Ma Y, Marie A, Andrieu J-P, Bedouet L, Feng Q. Proteomic and profile analysis of the proteins laced with aragonite and vaterite in the freshwater mussel *Hyriopsis cumingii* shell biominerals. Protein and Peptide Letters. 2013; 20 (10) :1170–1180. [PubMed: 23409939]

[80]. Pote KG, Ross MD. Each otoconia polymorph has a protein unique to that polymorph. Comparative Biochemistry and Physiology B, Comparative Biochemistry. 1991; 98 (2–3) :287–295. [PubMed: 1873986]

[81]. Mass T, Drake JL, Peters EC, Jiang W, Falkowski PG. Immunolocalization of skeletal matrix proteins in tissue and mineral of the coral *Stylophora pistillata* . Proceedings of the National Academy of Sciences. 2014; 111 (35) :12728–12733.

[82]. Coronado I, Fine M, Bosellini FR, Stolarski J. Impact of ocean acidification on crystallographic vital effect of the coral skeleton. Nature Communications. 2019; 10 (1) :1–9.

[83]. Konopacka-Lyskawa D. Synthesis methods and favorable conditions for spherical vaterite precipitation: A review. Crystals. 2019; 9 (4) :223.

[84]. Conci N, Wörheide G, Vargas S. New non-bilaterian transcriptomes provide novel insights into the evolution of coral skeletomes. Genome Biology and Evolution. 2019; 11 (11) :3068–3081. [PubMed: 31518412]

[85]. Gabay Y, Fine M, Barkay Z, Benayahu Y. Octocoral tissue provides protection from declining oceanic pH. PLoS ONE. 2014; 9 (4) e91553 [PubMed: 24710022]

[86]. Sammarco P, Coll J, La Barre S, Willis B. Competitive strategies of soft corals (Coelenterata: Octocorallia): allelopathic effects on selected scleractinian corals. Coral Reefs. 1983; 1 (3) :173–178.

[87]. Al-Rousan S, Pätzold J, Al-Moghrabi S, Wefer G. Invasion of anthropogenic CO_2 recorded in planktonic foraminifera from the northern Gulf of Aqaba. International Journal of Earth Sciences. 2004; 93 (6) :1066–1076.

[88]. Osman EO, Smith DJ, Ziegler M, Kürten B, Conrad C, El-Haddad KM, Voolstra CR, Suggett DJ. Thermal refugia against coral bleaching throughout the northern Red Sea. Global Change Biol. 2018; 24 (2) :e474–e484.

[89]. Loeppky AR, Belding LD, Quijada-Rodriguez AR, Morgan JD, Pracheil BM, Chakoumakos BC, Anderson WG. Influence of ontogenetic development, temperature, and pCO_2 on otolith calcium carbonate polymorph composition in sturgeons. Scientific Reports. 2021; 11 (1) :1–10. [PubMed: 33414495]

[90]. Holmberg RJ, Wilcox-Freeburg E, Rhyne AL, Tlusty MF, Stebbins A, Nye SW Jr, Honig A, Johnston AE, San Antonio CM, Bourque B. Ocean acidification alters morphology of all otolith types in Clark's anemonefish (*Amphiprion clarkii*). PeerJ. 2019; 7 e6152 [PubMed: 30643693]

[91]. Conci N, Lehmann M, Vargas S, Wörheide G. Comparative proteomics of octocoral and scleractinian skeletomes and the evolution of coral calcification. Genome Biology and Evolution. 2020; 12 (9) :1623–1635. [PubMed: 32761183]

[92]. Chen Z, Xin M, Li M, Xu J, Li X, Chen X. Biomimetic synthesis of coexistence of vaterite-calcite phases controlled by histidine-grafted-chitosan. Journal of Crystal Growth. 2014; 404 :107–115.

Europe PMC Funders Author Manuscripts

Statement of Significance

Vaterite is typically considered to be a metastable polymorph of calcium carbonate. While calcium carbonate structures formed within the tissues of octocorals (phylum Cnidaria), have previously been reported to be composed of the more stable polymorphs aragonite and calcite, we observed that vaterite dominates the mineralogy of sclerites of *Ovabunda macrospiculata* from the Red Sea. Based on electron microscopy, Raman spectroscopy, and X-ray diffraction analysis, vaterite appears to be the dominant polymorph in sclerites both in the tissue and after extraction and preservation. Although this is the first documentation of vaterite in soft coral sclerites, it likely will be found in sclerites of other related taxa as well.

Europe PMC Funders Author Manuscripts

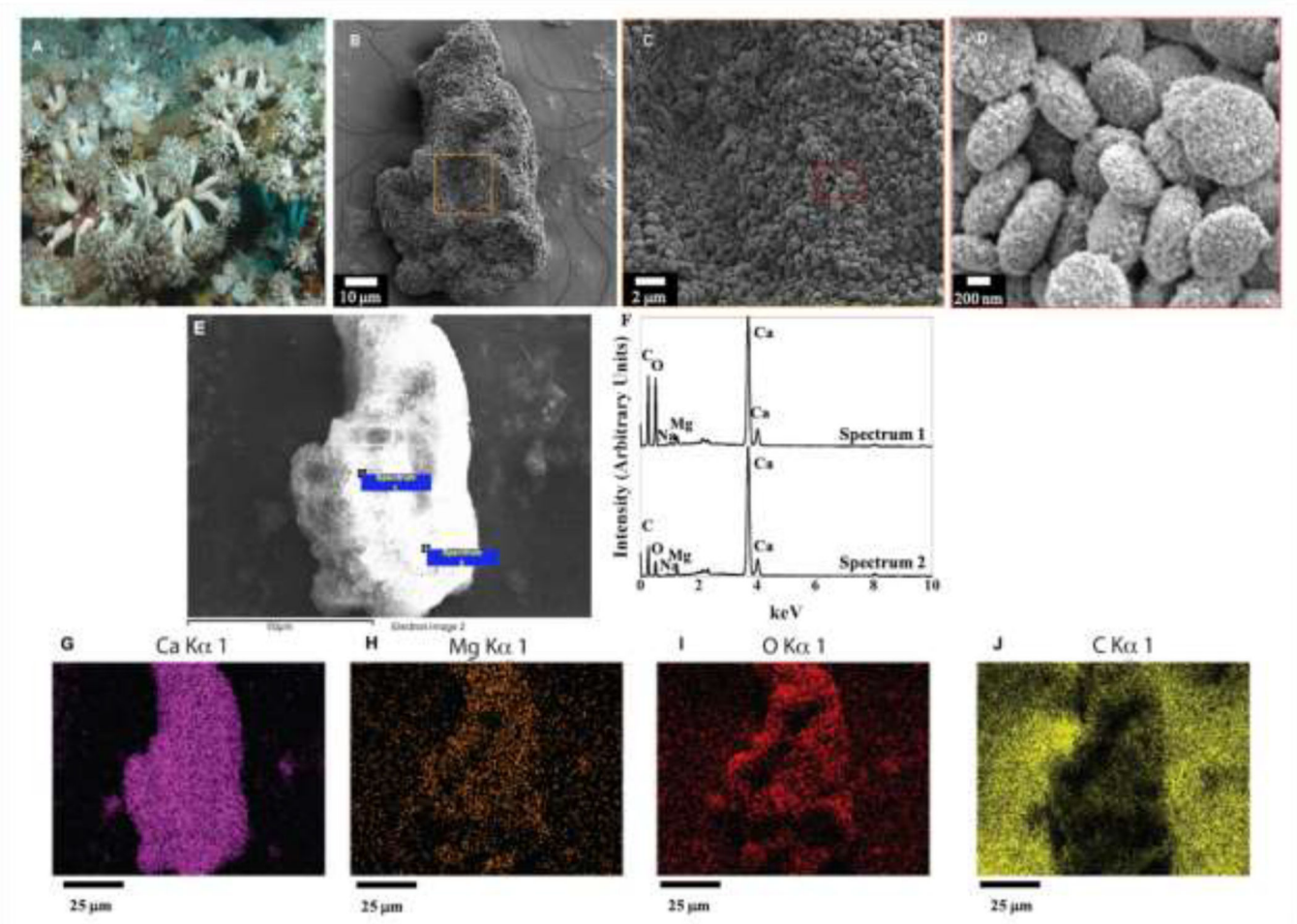

Figure 1. *Ovabunda macrospiculata* colony with extended polyps and tentacles

(A). SEM images of aggregated *O. macrospiculata* sclerites (B). Magnified image of microscleres at the surface of the sclerites (C is the inset orange box on B, D is the inset red box on C). EDS mapping of (B) showing the distribution of calcium, magnesium, oxygen, and carbon in the sclerite (G-J). Photo credit for (A): Ronen Liberman, Tel Aviv University.

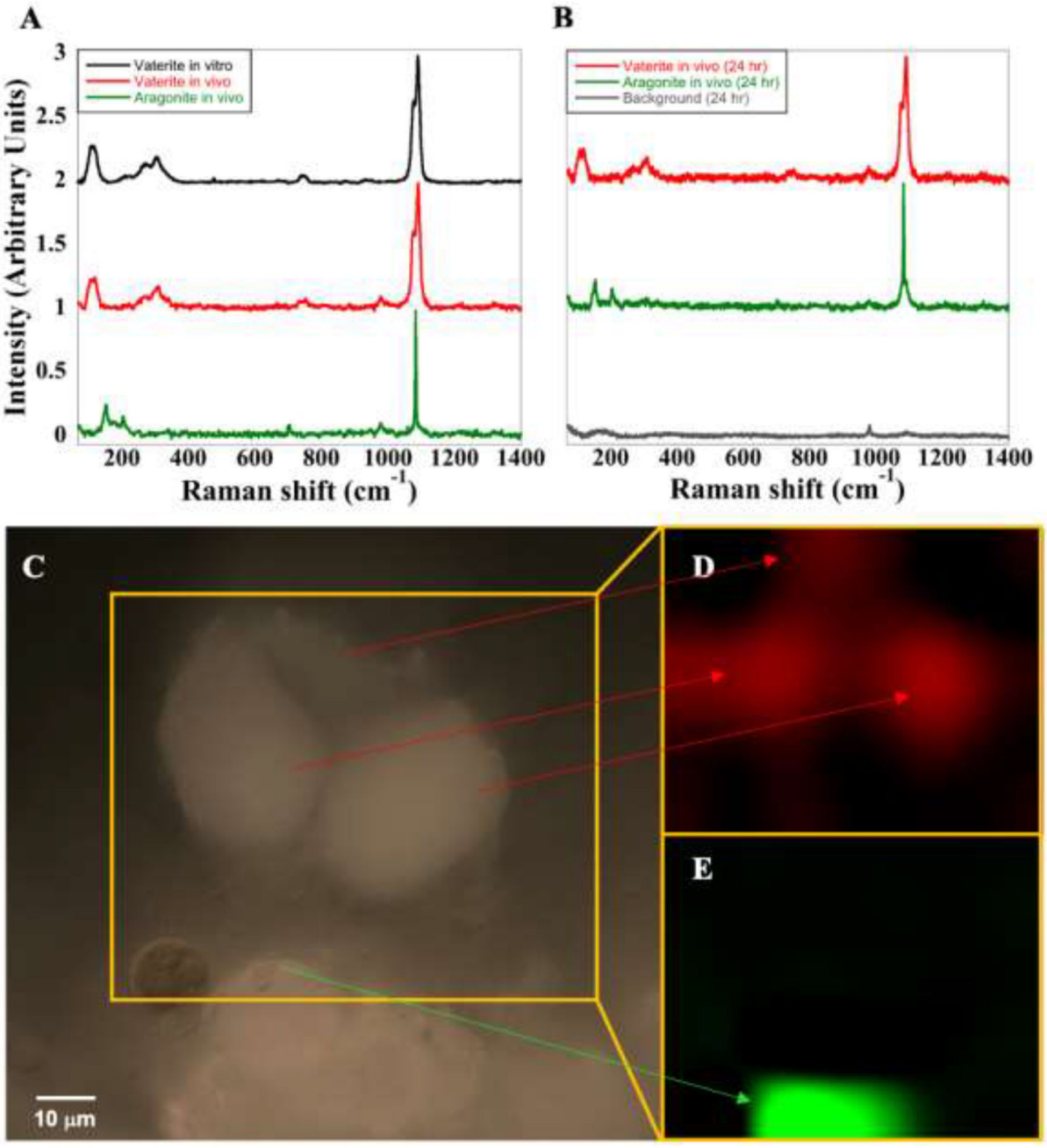

Figure 2. Micro-Raman spectroscopic mineral determination of isolated (A) and embedded (B) sclerites.

(A) Vaterite (black) was observed in a fixed sample of an *O. macrospiculata* sclerite isolated from the tissue. Vaterite (red) and aragonite (green) were observed in an *in-vivo* sclerite embedded in live tissue of *O. macrospiculata*. (B) The same colony was re-examined *in-vivo* after 24 hours, with vaterite (red) and aragonite (green) still detected. A small peak observed at ~980 cm^{-1} in all *in-vivo* measurements is likely sulfate from the surrounding seawater (panel B, gray spectrum). (C) Light micrograph with mapped locations of vaterite (red, D) and aragonite (green, E) within polyp tissue. D and E are the same locations in C noted by

the orange box. Arrows denote specific features of C observed by Raman spectroscopy to be vaterite (D) or aragonite (E).

Europe PMC Funders Author Manuscripts

Europe PMC Funders Author Manuscripts

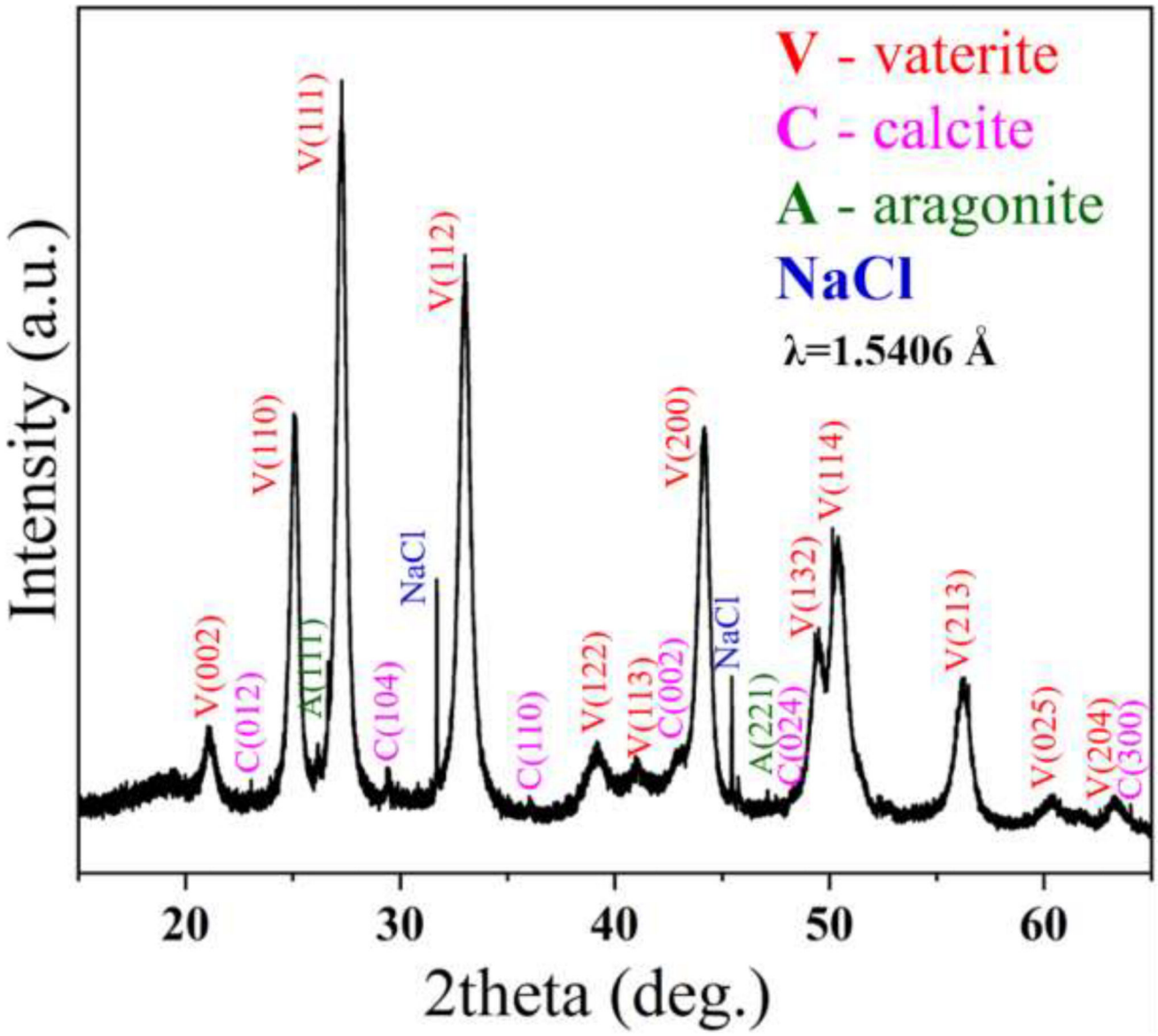

Figure 3. HRPXRD analysis of isolated sclerites reveals that they are predominantly vaterite (red), with much smaller amounts of calcite (pink), aragonite (green), and potentially halite (blue).